International Urogynecology Journal (2019) 30:977–984
https://doi.org/10.1007/s00192-019-03872-6

ORIGINAL ARTICLE

Signs of damage in pelvic floor muscles at the end of pregnancy in rabbits

Octavio Sánchez-García[1,2] · Laura G. Hernández-Aragón[1,3] · Kenia López-García[4] · Margarita Juárez[1] · Margarita Martínez-Gómez[1,4] · Francisco Castelán[1,4]

Received: 17 September 2018 / Accepted: 8 January 2019 / Published online: 1 February 2019

Abstract

Introduction and hypothesis Temporary effects to pelvic floor muscles are linked to impairments in micturition, particularly stress urinary incontinence (SUI), during pregnancy. We hypothesize that bulbospongiosus (Bsm) and pubococcygeus (Pcm) are differently damaged in primigravid and primiparous rabbits.

Methods Twenty-four rabbits allocated evenly ($n = 6$) into nulliparous, pregnant, and primiparous groups on postpartum days 3 (P3) and 20 (P20) were used to evaluate the myofiber cross-sectional area (CSA), β-glucuronidase activity, and anti-3-nitrotyrosine (anti-3-NTyr) immunoreactivity in Bsm and Pcm muscles. Appropriate statistical tests were done to determine significant differences among groups ($P \leq 0.05$).

Results The average CSA of Bsm was not significantly different, albeit a high percentage of myofibers was enlarged in late-pregnant and primiparous rabbits on P3; β-glucuronidase activity and indirect parameter of muscle damage was also higher. These variables did not change in the Pcm muscle during the different reproductive stages. In contrast, the 3-NTyr immunoreactivity, an indicator of oxidative damage, was increased on P3 for Pcm myofibers and P20 for myofibers of both muscles.

Conclusions Our findings demonstrate reliable signs of damage to Bsm and Pcm muscles in young female rabbits passing different reproductive stages. Damage to the Bsm muscles as detected at the end of pregnancy persisted after delivery. This was not the case for Pcm muscles, in which damage seems to appear after delivery.

Keywords Bulbospongiosus muscle · Pubococcygeus muscle · Inflammation · Primiparity · Reproduction

Octavio Sánchez-García and Laura G. Hernández-Aragón contributed equally to this work.

Work done at the Unidad Foránea Tlaxcala, Instituto de Investigaciones Biomédicas, Universidad Nacional Autónoma de México in the Centro Tlaxcala de Biología de la Conducta, Universidad Autónoma de Tlaxcala

✉ Francisco Castelán
fcocastelan@iibiomedicas.unam.mx

[1] Centro Tlaxcala de Biología de la Conducta, Universidad Autónoma de Tlaxcala, Tlaxcala, Mexico

[2] Departamento de Biología y Toxicología de la Reproducción, Instituto de Ciencias, Benemérita Universidad Autónoma de Puebla, Puebla, Mexico

[3] Instituto de Fisiología, Benemérita Universidad Autónoma de Puebla, Puebla, Mexico

[4] Departamento de Biología Celular y Fisiología, Instituto de Investigaciones Biomédicas, Universidad Nacional Autónoma de México, Mexico City, Mexico

Abbreviations

3-NTyr	3-nitrotyrosine
ANOVA	Analysis of variance
Bsm	Bulbospongiosus muscle
CSA	Cross-sectional area
EUS	External urethral sphincter
H&E	Hematoxylin–eosin
LSC	Ligament suspensory of clitoris
LUT	Lower urogenital tract
NO	Nitric oxide
NOS	Nitric oxide synthase
Pcm	Pubococcygeus muscle
PFM	Pelvic floor muscles
PMN	Polymorphonuclear
ROS	Reactive oxygen species
SUI	Stress urinary incontinence
Th cells	T helper cell types.

Introduction

Pelvic floor muscles (PFM) assist the lower urogenital tract (LUT) in reproductive and excretory functions. Pregnancy and childbirth are major risk factors for the development of stress urinary incontinence (SUI) and pelvic organ prolapse (POP) in women. Labor trauma is generally assumed as the core of PFM impairments, albeit the contribution of pregnancy remains to be more thoroughly addressed. Transitory effects to PFM are linked to impairments in sexual function and micturition, including the onset of SUI during pregnancy [1–3]. Indeed, individual PFM can assist differently in urinary continence and voiding [4, 5]. Studies conducted in rats have contributed to understand the effect of pregnancy on the PFM, e.g., pubococcygeus (Pcm), iliococcygeus, and coccygeus muscles, but its participation in micturition is unknown [6–8]. The LUT in domestic female rabbits is associated with well-defined pelvic (pubococcygeus; Pcm) and perineal (bulbospongiosus; Bsm) muscles that exhibit reflex activation at the voiding and storage phases of micturition, respectively [9–11]. This synchronous activation is lost in multiparous rabbits that display urodynamic alterations likely related to neural and muscular damage [12–15]. The Bsm and Pcm of multiparous rabbits show asymmetric processes of damage, as supported by β-glucuronidase activity [16]. Multiparity implies repeated and successive deliveries, making it impossible to determine the extent to which pregnancy and primiparity influence muscle damage. Overall, we hypothesized that the Bsm and Pcm are differently damaged in primigravid and primiparous rabbits.

The main objective of this study was to evaluate the effect of pregnancy and primiparity on histological and biochemical parameters related to muscle damage in the Bsm and Pcm of nulliparous, late-pregnant, and primiparous rabbits on postpartum days 3 (P3) and 20 (P20). To this end, we sought to identify histopathological signs of damage in hematoxylin–eosin (H&E)-stained sections, measured β-glucuronidase activity, and estimated the presence of 3-nitrotyrosine (3-NTyr) as a reliable marker related to reactive oxygen species (ROS).

Materials and methods

Animals

Twenty-four young (6-month-old) chinchilla-breed female rabbits (*Oryctolagus cuniculus*) were housed in individual stainless-steel cages and kept at 20 ± 2 °C under artificial lighting conditions (L: D 16:8, lights on at 0600 h). They were daily provided with pellet food (Conejina, Purina, México) and continuous access to water. The Ethics Committee from the Universidad Autónoma de Tlaxcala approved all experimental procedures listed below.

Rabbits were divided into nulliparous (N, $n = 6$), late-pregnant (G, $n = 6$), and primiparous (P, $n = 12$) groups. With the exception of rabbits in the N group that were not mated, all females were mated at 6 months of age. Group G rabbits were euthanized 30 days postmating (pregnancy lasts ~31 days); the pups were surgically extracted and decapitated. The primiparas were euthanized on P3, ($n = 6$) or P20 ($n = 6$); the pups were decapitated on P1 [17]. The rabbits in group N were sacrificed at 7 months old. All were euthanized with an overdose of sodium pentobarbital (100 mg/kg i.p., Pfizer).

Sample processing

Dissection of the Bsm and Pcm was done as described elsewhere [18]. Briefly, a midline incision was made from the abdomen to the perineal vagina, and abdominal muscles and adipose tissue were removed to dissect the Bsm. Ischium and pubis bones were removed to dissect the Pcm. The right Pcm muscles were histologically processed and the left ones used to measure β-glucuronidase activity. For the Bsm, we used both muscles (right and left) together, as reported elsewhere [18]. These were cut at midline to obtain two segments; the rostral one was processed for histological analysis, while the caudal one was used to measure β-glucuronidase activity. Muscles collected to analyze enzymatic activity were immediately frozen and stored at 80 °C until assayed. The Bsm and Pcm were measured in their length and width, excised, and weighed.

General histology

Muscles were placed into a plastic holder and immersed in Bouin-Duboscq fixative for 24 h at room temperature. After embedding in paraplast-Xtra (Sigma-Aldrich), 7-μm-thick transverse sections were obtained with a microtome (RM2135, Leica) mounting in a series of four sections per slide. The fifth slide was stained with H&E. Slides were covered with mounting medium (Cytoseal 60, Richard-Allan Scientific) and a coverslip and observed with a microscope (Eclipse Ni, Nikon). Images were acquired with a digital camera (DS-Ri2, Nikon). Qualitative analysis was done by two independent observers (FC, LGHA) examining the same slide, on which the CSA was measured (*see* below).

Tissue analysis

Sections from the medial region of each muscle stained with H&E were observed at 400× magnification under light microscopy, and four digital photomicrographs were obtained from the center of each section. For each image, 12–13 fibers were randomly selected to measure the cross-sectional area (CSA) [18]. These were sampled by using a grid (6 × 4 quadrants) placed over the screen of a desktop computer displaying

the image [6]. The CSA of 50 fibers were counted per muscle section per rabbit with the program AxioVision Rel 4.6 (Carl Zeiss).

β-glucuronidase assays

The extent of muscle damage was assessed measuring β-glucuronidase activity [16]. Briefly, ~100 mg of each muscle was used to prepare total protein extracts in lysis buffer [20 mM Tris-hydrochloric acid (HCl pH 7.4, 100 mM glycine, 100 mM sodium chloride (NaCl), 0.1% triton X-100, 1 mM phenylmethylsulfonyl fluoride, 1 mM DL-dithiothreitol] added to a protease inhibitor cocktail (Sigma-Aldrich). Supernatants were incubated with 5 mM p-nitrophenyl-b-D-glucuronide (Sigma–Aldrich) as the enzyme substrate [16, 19]. After enzymatic reaction was stopped, β-glucuronidase activity was measured by spectrophotometry using p-Nitrophenol (4-nitrophenol, Sigma–Aldrich) to build a standard curve. Samples and standards were measured in duplicate at 420 nm.

Immunohistochemistry

Sets of homologous slides from each experimental group were simultaneously processed to estimate the 3-NTyr immunostained area [20]. Briefly, slides were incubated overnight at 4 °C with the primary antibody (1:200, mouse monoclonal anti-3- NTyr; cat. MAB 5404; Chemicon Millipore), followed by incubation with a secondary antibody [2 h at 4 °C; 1:250, goat anti-mouse immunoglobulin (IgG)-biotinylated; Vector Labs, USA]. Immunostaining was developed using the Vectastain ABC kit (Vector Labs, USA), and sections were counterstained with cresyl violet in due course. Sections were observed under light microscopy and photographed. The percentage of 3-NTyr immunoreactive area was calculated using the program Axio Vision Rel 4.6, as reported elsewhere for liver sections [20].

Statistical analyses

All measured variables are expressed as mean ± standard error of the mean (SEM). Data were not parted from a normal distribution as assessed using Kolmogorov-Smirnov tests. One-way analysis of variance (ANOVA) was followed by Newman-Keuls tests to determine significant differences among groups regarding bodily and macroscopic muscle variables, average CSA, β-glucuronidase activity, and percentage of 3-NTyr immunostained area in the Bsm and Pcm. To detect significant differences between the CSA according to fiber size bin and experimental manipulation, two-way ANOVA followed by Newman-Keuls tests was used. Statistical level of significance was set at $P \leq 0.05$. All statistical tests were done using the program Prism 6 for Mac (GraphPad Software).

Results

Body weight did not significantly differ between N, G, P3, and P20 groups (F = 1.761, $P = 0.187$; Table 1). The same was true for Bsm width (F = 0.5168, $P = 0.6755$). In contrast, Bsm length and normalized weight changed significantly between groups (F = 4.014, $P = 0.0218$). Post-hoc tests indicated a significant increase in Bsm length in G compared with N, while the opposite effect was found for G vs. P3 groups (Table 1). Otherwise, a significant decrease in normalized weight in G compared with P3 and P20 was observed (Table 1). For Pcm, normalized muscle weight (F = 1.274, $P = 0.3102$), length (F = 1.7, $P = 0.1992$), and width (F = 0.9842, $P = 0.4201$) were not significantly different between groups (Table 1).

Morphology of Bsm and Pcm

Both right and left Bsm were excised and maintained together, and the connective tissue between them was seen ventrally in all sections; nerve bundles were seen laterally next to blood vessels. In comparison with the N group, there was a remarkable presence of polymorphonuclear (PMN) cells and hypereosinophilic and rounded fibers in Bsm sections of the G and P3 groups (Fig. 1a–c). These characteristics were also present for the P20 group, albeit to a lesser extent (Fig. 1d).

The average CSA of Bsm myofibers was not significantly different between groups (F = 2.269, $P = 0.1117$; Fig. 1e). A further analysis of frequency distribution showed significant differences for the 500- and >1250-μm^2 CSA bins between groups (Fig. 1f). Thus, the percentage of fibers in the G group, with CSA ranging from 251 to 500 μm^2, was significantly lower than the N group. In contrast, the percentage of myofibers in the G group, with CSA >1250 μm^2, was significantly higher than the N group, while a significant decrease was identified between the P20 and P3 groups (Fig. 1f).

Capillaries of different calibers were seen next to the edge of Pcm myofibers. In addition, muscle spindles were seen in the periphery of the section. Muscle sections of the N group showed scant fields with PMN (Fig. 2a). In clear contrast, clusters of PMN cells were frequently observed in G-group sections. Furthermore, there was a scant presence of rounded myofibers (Fig. 2b). Clusters of PMN cells persisted in muscle sections of the P3 group, which also showed a moderate presence of rounded fibers (Fig. 2c). A moderate presence of PMN cells and round fibers was also seen in sections of the P20 group (Fig. 2d).

The average CSA of Pcm myofibers was not significantly different among the four experimental groups (Fig. 2e). The same was true for frequency distribution (Fig. 2f).

Table 1 Body weight and muscle morphometry of nulliparous (N), late-pregnant (G), and primiparous on postpartum days 3 (P3) and 20 (P20) rabbits

	N	G	P3	P20
Body weight (kg)	4.2 ± 0.1	3.9 ± 0.1	3.8 ± 0.2	3.8 ± 0.1
Bulbospongiosus muscle				
Length (mm)	15.7 ± 0.45	18.3 ± 0.66*	15 ± 1.06**	16.82 ± 0.48
Width (mm)	7.3 ± 0.19	7.5 ± 0.24	7.2 ± 0.14	7.2 ± 0.18
Normalized wet weight (mg/kg body weight)	67.2 ± 5.7	57.5 ± 5.9	88.3 ± 6.5**	84 ± 8.4***
Pubococcygeus muscle				
Length (mm)	29.5 ± 0.54	28.4 ± 0.28	29.7 ± 0.34	28.1 ± 0.93
Width (mm)	7.4 ± 0.29	7.1 ± 0.28	7 ± 0.16	6.85 ± 0.18
Normalized wet weight (mg/kg body weight)	71.5 ± 4.5	67.7 ± 3.13	71.5 ± 2.74	78.8 ± 5.6
Perineal vagina wet weight (mg)	36.6 ± 1.3	37 ± 2.1	40 ± 1.5	39.1 ± 1.7

*$P < 0.05$ G vs. N, **, $P < 0.05$ P3 vs. G, *** $P < 0.05$ P20 vs. G

β-glucuronidase activity of Bsm and Pcm

β-glucuronidase activity of the Bsm was significantly different between groups (F = 18.48, $P < 0.0001$). Post-hoc tests indicated that β-glucuronidase activity of the G group was higher than the N ($P < 0.001$) and P20 ($P < 0.001$; Fig. 3a) groups. Furthermore, β-glucuronidase activity of the P3 group was higher than in the N ($P < 0.001$) and P20 ($P < 0.001$). groups. β-glucuronidase activity for Pcm was not significantly different between groups (F = 2.74, $P = 0.0703$; Fig. 3b).

3-NTyr immunostaining of Bsm and Pcm

The 3-NTyr immunostaining in Bsm and Pcm sections was assessed as an indicator of protein oxidation (Fig. 4a–h). For Bsm, the percentage of 3-NTyr immunostaining was significantly different between groups (F = 4.198, $P = 0.0186$; Fig. 4i) and was significantly higher in the P20 ($P < 0.05$) than the N group; the remaining comparisons were not significant (Fig. 4i). For the Pcm, the percentage of 3-NTyr immunostaining was significantly different between groups (F = 5.654, $P = 0.0057$); post hoc tests indicated a significant increase in P3 and P20 vs. the N group ($P < 0.05$ and $P < 0.01$, respectively. Fig. 4j).

Discussion

Our findings demonstrate morphometric and biochemical alterations in the Bsm at the end of pregnancy, which include increase in muscle length, enlargement of CSA in some myofibers, and an increase in β-glucuronidase activity at the end of pregnancy. In late-pregnant rabbits, none of these variables were modified in the Pcm, in which there was an important presence of PMN cells. Furthermore, 20 days postpartum, there was an increase in the 3-NTyr immunostained area for the Bsm, while this was increased on P3 and P20 for the Pcm.

In rats, pregnancy is associated with a transitory increase in vaginal length and decrease in vaginal stiffness [21, 22]. These adaptations may help to avoid major vaginal injuries, albeit adjacent tissues displayed no matching responses. Late pregnancy increases pubocaudalis (also known as Pcm) and coccygeus muscle stiffness but decreases it in iliococcygeus muscles [6, 7]. Such information could be helpful to explain differences regarding Bsm and Pcm injuries in late-pregnant rabbits: The fact that the Bsm is inserted into the ligament suspensory of clitoris (LSC), ventrally on the perineal (lower) vagina [9], increases its susceptibility to straining injuries due to a possible vaginal elongation in late pregnancy. In contrast, the Pcm is not adjoined to the vagina in rabbits [7]. Otherwise, a differential increase in muscle stiffness, as shown for the Pcm in female rats [6], may protect it against injuries at the end of pregnancy. These adaptations may not occur in the Bsm, and changes affecting the connective tissue of the LSC would thus contribute to straining injuries in late-pregnant rabbits. Overall, macroscopic variables suggest the Bsm is more severely damaged than the Pcm during late pregnancy.

In clear contrast with the Bsm, we observe a remarkable presence of PMN cells in the Pcm at the end of pregnancy that persisted on P3. Certainly, in women, pro- and anti-inflammatory actions are involved in the beginning and mid- to late-term pregnancy, respectively [23]. Some proinflammatory actions in peripheral blood and in the maternal–fetal interface involve T helper cells (Th cells) actions that reflect proinflammatory, anti-inflammatory, and proinflammatory states at early, mid-, and late-pregnancy stages, respectively [23]. Indeed, the proinflammatory state related to labor trauma in which Th and PMN cells (e.g., neutrophils and macrophages) participate seems highly important to a cell-based secondary prevention of childbirth-induced pelvic floor trauma [24]. Overall, findings herein highlight the need to evaluate the immune response related with pregnancy in PFM to understand pelvic floor dysfunctions linked to pregnancy and childbirth.

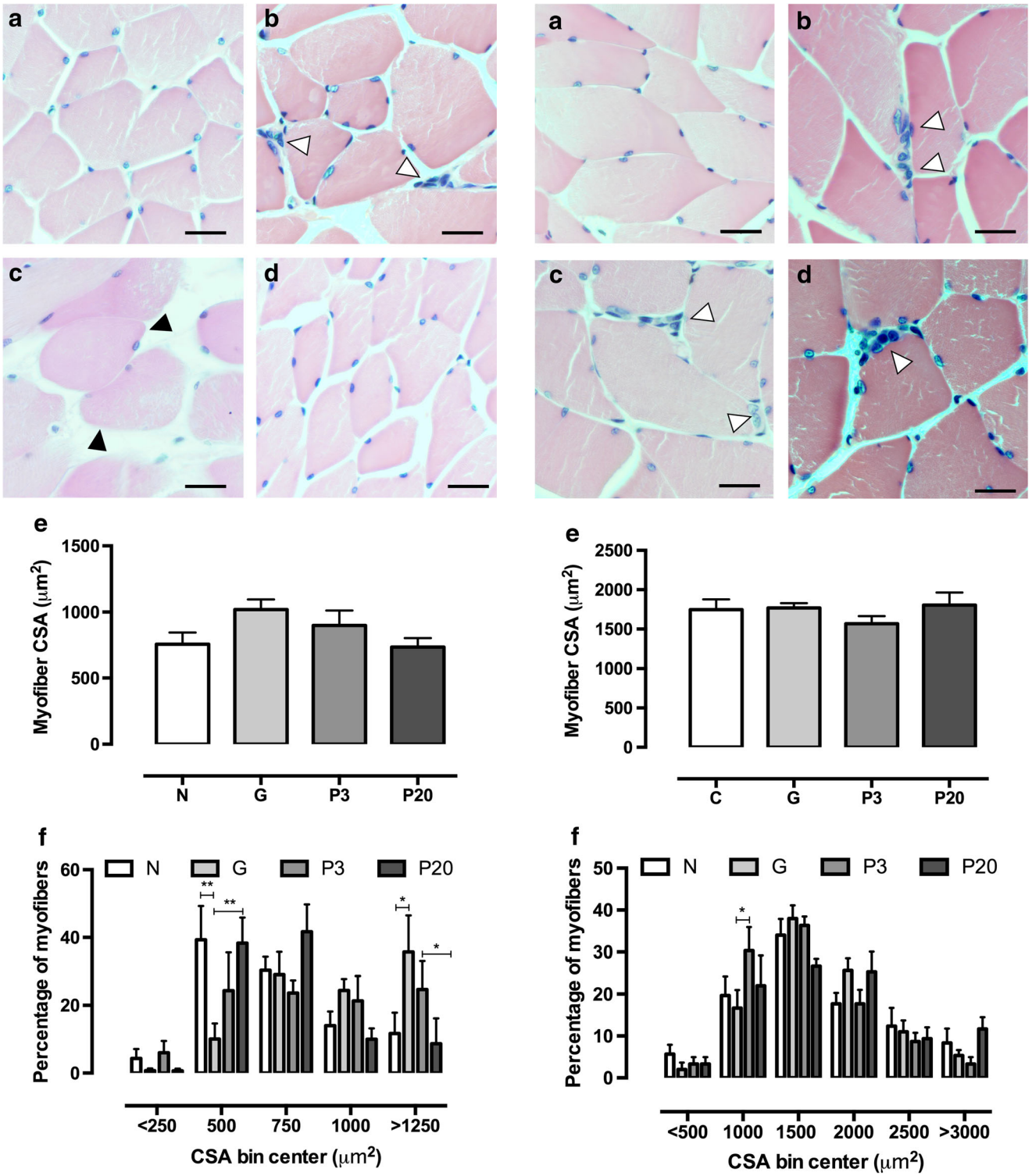

Fig. 1 Morphometrical characteristics of bulbospongiosus (Bsm) myofibers from nulliparous (N; **a**), late-pregnant (G; **b**), and primiparous on postpartum days 3 (P3; **c**) and 20 (P20; **d**) rabbits. Muscle sections were stained with hematoxylin–eosin. Average cross-sectional area (CSA; **e**) and CSA distribution of myofibers (**f**). Data are means ± standard errors (*$P < 0.05$; **,$P < 0.01$). *White arrowheads*, polymorphonuclear (PMN) cells; *black arrowheads*, round fibers. *Scale bars*, 20 μm

Fig. 2 Morphometrical characteristics of pubococcygeus (Pcm) myofibers from nulliparous (N; **a**), late-pregnant (G; **b**), and primiparous on postpartum days 3 (P3; **c**) and 20 (P20; **d**) rabbits. Muscle sections were stained with hematoxylin-eosin. Average cross-sectional area (CSA; **e**) and CSA distribution of myofibers (**f**). Data are means ± standard errors. *$P < 0.05$. *White arrowheads* polymorphonuclear (PMN) cells. *Scale bars*, 20 μm

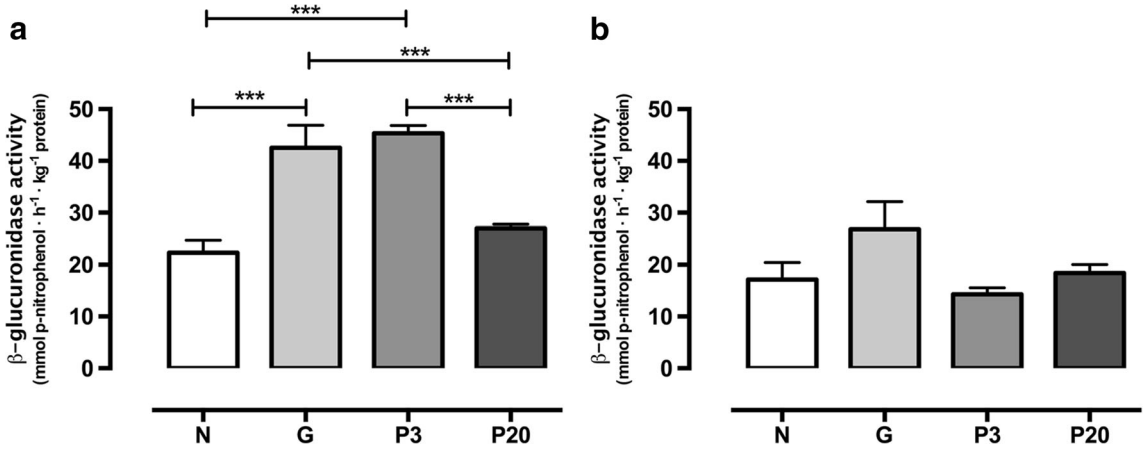

Fig. 3 β-glucuronidase activity in bulbospongiosus (Bsm; **a**) and pubococcygeus (Pcm; **b**) muscles from nulliparous (N), late-pregnant (G), and primiparous on postpartum days 3 (P3) and 20 (P20) rabbits. Data are means ± standard errors. ***$P < 0.001$

For skeletal muscle, a direct proportion between myofiber CSA and contractile force is generally assumed. Nevertheless, the transient increase in myofiber CSA could also be considered a sign of muscle damage related to edema [25]. Indeed, the increase in the CSA of Pcm myofibers is related to muscle damage in multiparous rabbits [16]. Our findings show that pregnancy leads to a transient reduction in the percentage of Bsm myofibers with a CSA ranging from 251 to 500 μm^2,

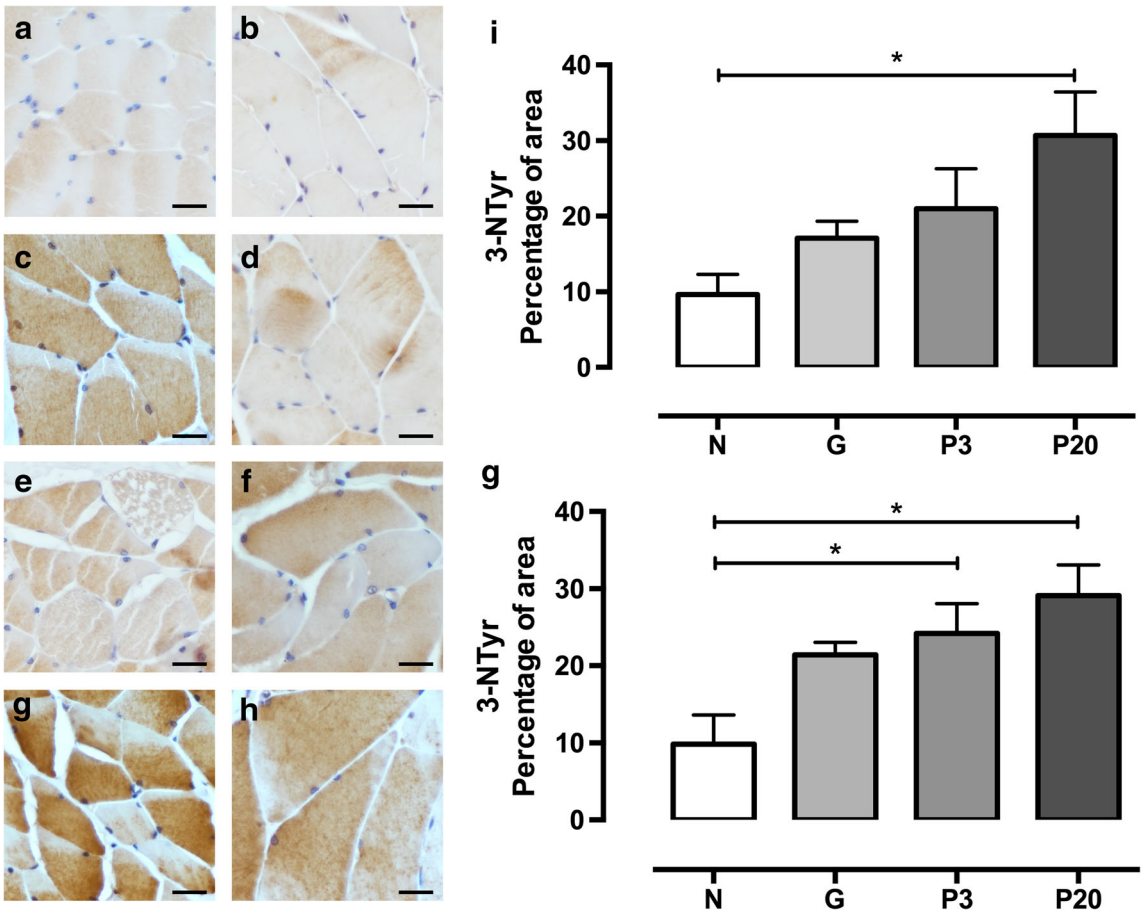

Fig. 4 3-nitrotyrosine (3-NTyr) immunostained sections of the bulbospongiosus (Bsm; **a**, **c**, **e**, **g**) and pubococcygeus (Pcm; **b**, **d**, **f**, **h**, **j**) muscles from nulliparous (N; **a**, **b**), late-pregnant (G; **c**, **d**), and primparous on postpartum days 3 (P3; **e**, **f**) and 20 (P20; **g**, **h**) rabbits. Data are means ± standard error of the 3-NTyr immunostained area, expressed percentage for Bsm (**i**) and Pcm (**j**). *$P < 0.05$

which matches with a high percentage of myofibers with CSA >1250 μm^2 reverted on P20. Such findings suggest that a subpopulation of myofibers could be predominantly affected (i.e., glycolytic and type II fibers in the Bsm are more abundant than in the Pcm [14]). No similar alterations were observed for Pcm myofibers either on late-pregnancy or postpartum stage. Indeed, pregnancy in rats induces transient adaptations involving contractile properties (i.e., addition of sarcomeres and high physiological CSA) and connective tissue (i.e., collagen content), which could preclude injuries in the Pcm due to delivery [6–8].

Data regarding β-glucuronidase activity, an indirect marker of global muscle damage [12], support the notion that damage in the Bsm is detected from late pregnancy and persists on P3. In contrast, activity measured in the Pcm did not support evidence for damage either in pregnancy or the postpartum stage. These biochemical findings do not agree with histological ones, possibly due to the muscle portion used for each case. Otherwise, β-glucuronidase activity in the Bsm and Pcm, and hence the extent of damage, in primiparous rabbits is opposed to that in multiparous rabbits [16]. Therefore, it could be hypothesized that PFM damage related to repeated episodes of pregnancy and delivery in multiparous rabbits is not merely cumulative.

The abundance of 3-NTyr is considered an indirect marker of oxidative stress in skeletal muscle [26]. Following the elevation in ROS, resulting peroxynitrites could react with nitric oxide (NO) to produce and accumulate 3-NTyr inside muscles [27, 28]. The intensity of 3-NTyr immunostaining observed in sections from the Bsm and Pcm of primiparas at P3 (Pcm) and P20 (Bsm and Pcm) supports the notion that delivery causes oxidative damage in the Bsm and Pcm. Considering that vaginal distention in rats causes a transient blood-flow occlusion affecting the external urethral sphincter (EUS) [29], delivery in rabbits may occlude blood flow in the Bsm and Pcm, which could elevate muscle ROS. Such a proposal would be useful to explain only the 3-NTyr immunostaining in the Pcm on P3, given the temporal course of oxidative damage following an ischemia/reperfusion event. The fact that the Pcm is composed mainly of oxidative fibers supports this notion [14]. The higher 3-NTyr immunoreactive area in sections from the Bsm and Pcm on P20 may be related to elevated levels of NO involving, possibly, an upregulation of NOS expression that has been linked to muscle regeneration [27, 28].

The main limitation of this study is the lack of approaching plausible alterations in contractility of the Bsm and Pcm and in muscle reflex activation during micturition, which would have given information about alterations in voiding or continence of urine [11]. In clear difference to women, in whom the growing womb compresses the pelvic floor, signs of damage in female rabbit PFM, a quadruped species, suggest that hormone milieu due to pregnancy is involved in postpartum stage remodeling. Despite inherent differences regarding PFM anatomy between rabbits and women, pregnancy is considered an inflammatory state [23, 30]. This should be further evaluated to advance our knowledge about PFM damage and plasticity during reproduction.

Acknowledgements The authors thank Jesus Ramses Chávez Ríos and Laura García Rivera for their excellent technical assistance. This study was partially granted by the Consejo Nacional de Ciencia y Tecnología of México (Infraestructura 225126) to the Cuerpo Académico de Fisiología del Comportamiento (MMG, FC).

Compliance with ethical standards

Conflicts of interest None.

References

1. Elenskaia K, Thakar R, Sultan AH, et al. The effect of pregnancy and childbirth on pelvic floor muscle function. Int Urogynecol J. 2011;22:1421–7. https://doi.org/10.1007/s00192-011-1501-5.
2. Tennfjord MK, Hilde G, Stær-Jensen J, et al. Dyspareunia and pelvic floor muscle function before and during pregnancy and after childbirth. Int Urogynecol J. 2014;25:1227–35. https://doi.org/10.1007/s00192-014-2373-2.
3. Martínez Franco E, Parés D, Lorente Colomé N, et al. Urinary incontinence during pregnancy. Is there a difference between first and third trimester? Eur J Obstet Gynecol Reprod Biol. 2014;182:86–90. https://doi.org/10.1016/j.ejogrb.2014.08.035.
4. Deindl FM, Vodusek DB, Hesse U, Schüssler B. Pelvic floor activity patterns: comparison of nulliparous continent and parous urinary stress incontinent women. A kinesiological EMG study. Br J Urol. 1994;73:413–7.
5. Shafik A, Shafik AA, Sibai El O, Shafik IA. Effect of micturition on clitoris and cavernosus muscles: an electromyographic study. Int Urogynecol J Pelvic Floor Dysfunct. 2008;19:531–5. https://doi.org/10.1007/s00192-007-0471-0.
6. Alperin M, Kaddis T, Pichika R, et al. Pregnancy-induced adaptations in intramuscular extracellular matrix of rat pelvic floor muscles. Am J Obstet Gynecol. 2016;215:210.e1–7. https://doi.org/10.1016/j.ajog.2016.02.018.
7. Alperin M, Lawley DM, Esparza MC, Lieber RL. Pregnancy-induced adaptations in the intrinsic structure of rat pelvic floor muscles. Am J Obstet Gynecol. 2015;213:191.e1–7. https://doi.org/10.1016/j.ajog.2015.05.012.
8. Catanzarite T, Bremner S, Barlow CL, et al. Pelvic muscles' mechanical response to strains in the absence and presence of pregnancy-induced adaptations in a rat model. Am J Obstet Gynecol. 2018;218:512.e1–9. https://doi.org/10.1016/j.ajog.2018.02.001.
9. Cruz Y, Hudson R, Pacheco P, et al. Anatomical and physiological characteristics of perineal muscles in the female rabbit. Physiol Behav. 2002;75:33–40.
10. Cruz Y, Corona-Quintanilla DL, Juárez M, Martínez-Gómez M. Características anatómicas y fisiológicas de los músculos pélvicos en la coneja doméstica (Oryctolagus cuniculus). Vet Mex. 41:263–74.
11. Corona-Quintanilla DL, Castelán F, Fajardo V, et al. Temporal coordination of pelvic and perineal striated muscle activity during

micturition in female rabbits. J Urol. 2009;181:1452–8. https://doi.org/10.1016/j.juro.2008.10.103.
12. Castelán F, López-García K, Moreno-Pérez S, et al. Multiparity affects conduction properties of pelvic floor nerves in rabbits. Brain Behav. 2018;8:e01105. https://doi.org/10.1002/brb3.1105.
13. Martínez-Gómez M, Mendoza-Martínez G, Corona-Quintanilla DL, et al. Multiparity causes uncoordinated activity of pelvic- and perineal-striated muscles and urodynamic changes in rabbits. Reprod Sci. 2011;18:1246–52. https://doi.org/10.1177/1933719111411728.
14. López-García K, Mariscal-Tovar S, Serrano-Meneses MA, et al. Fiber type composition of pubococcygeus and bulbospongiosus striated muscles is modified by multiparity in the rabbit. Neurourol Urodyn. 2017;36:1456–63. https://doi.org/10.1002/nau.23143.
15. López-Juárez R, Zempoalteca R, Corona-Quintanilla DL, et al. Multiparity modifies contractile properties of pelvic muscles affecting the genesis of vaginal pressure in rabbits. Neurourol Urodyn. 2017;98(1). https://doi.org/10.1002/nau.23305.
16. López-García K, Cuevas E, Sánchez-García O, et al. Differential damage and repair responses of pubococcygeus and bulbospongiosus muscles in multiparous rabbits. Neurourol Urodyn. 2016;35:180–5. https://doi.org/10.1002/nau.22702.
17. García-Villamar V, Hernández-Aragón LG, Chávez-Ríos JR, et al. Expression of glial cell line-derived neurotrophic factor (GDNF) and the GDNF family receptor alpha subunit 1 in the paravaginal ganglia of nulliparous and primiparous rabbits. Int Neurourol J. 2018;22:S23–33. https://doi.org/10.5213/inj.1834974.487.
18. López-García K, Cuevas E, Corona-Quintanilla DL, et al. Effect of multiparity on morphometry and oestrogen receptor expression of pelvic and perineal striated muscles in rabbits: is serum oestradiol relevant? Eur J Obstet Gynecol Reprod Biol. 2013;169:113–20. https://doi.org/10.1016/j.ejogrb.2013.03.032.
19. Komulainen J, Kytölä J, Vihko V. Running-induced muscle injury and myocellular enzyme release in rats. J Appl Physiol. 1994;77:2299–304. https://doi.org/10.1152/jappl.1994.77.5.2299.
20. Nicolás-Toledo L, Cervantes-Rodríguez M, Cuevas-Romero E, et al. Hitting a triple in the non-alcoholic fatty liver disease field: sucrose intake in adulthood increases fat content in the female but not in the male rat offspring of dams fed a gestational low-protein diet. J Dev Orig Health Dis. 2018;9:151–9. https://doi.org/10.1017/S204017441700099X.
21. Rundgren A. Physical properties of connective tissue as influenced by single and repeated pregnancies in the rat. Acta Physiol Scand Suppl. 1974;417:1–138.
22. Feola A, Moalli P, Alperin M, et al. Impact of pregnancy and vaginal delivery on the passive and active mechanics of the rat vagina. Ann Biomed Eng. 2011;39:549–58. https://doi.org/10.1007/s10439-010-0153-9.
23. Kalagiri RR, Carder T, Choudhury S, et al. Inflammation in complicated pregnancy and its outcome. Am J Perinatol. 2016;33:1337–56. https://doi.org/10.1055/s-0036-1582397.
24. Callewaert G, Da Cunha MMCM, Sindhwani N, et al. Cell-based secondary prevention of childbirth-induced pelvic floor trauma. Nat Rev Urol. 2017;14:373–85. https://doi.org/10.1038/nrurol.2017.42.
25. Damas F, Phillips SM, Lixandrão ME, et al. Early resistance training-induced increases in muscle cross-sectional area are concomitant with edema-induced muscle swelling. Eur J Appl Physiol. 2016;116:49–56. https://doi.org/10.1007/s00421-015-3243-4.
26. Buchwalow IB, Minin EA, Müller F-U, et al. Nitric oxide synthase in muscular dystrophies: a re-evaluation. Acta Neuropathol. 2006;111:579–88. https://doi.org/10.1007/s00401-006-0069-5.
27. Stamler JS, Meissner G. Physiology of nitric oxide in skeletal muscle. Physiol Rev. 2001;81:209–37. https://doi.org/10.1152/physrev.2001.81.1.209.
28. Pearson SJ, Hussain SR. A review on the mechanisms of blood-flow restriction resistance training-induced muscle hypertrophy. Sports Med. 2015;45:187–200. https://doi.org/10.1007/s40279-014-0264-9.
29. Damaser MS, Whitbeck C, Chichester P, Levin RM. Effect of vaginal distension on blood flow and hypoxia of urogenital organs of the female rat. J Appl Physiol. 2005;98:1884–90. https://doi.org/10.1152/japplphysiol.01071.2004.
30. Hung T-H, Lo L-M, Chiu T-H, et al. A longitudinal study of oxidative stress and antioxidant status in women with uncomplicated pregnancies throughout gestation. Reprod Sci. 2010;17:401–9. https://doi.org/10.1177/1933719109359704.